

## Deposition of Multicomponent Chromium Carbide Coatings Using a Non-Conventional Source of Chromium and Silicon with Micro-Additions of Boron

Jesús Eduardo González Ruiz<sup>a\*</sup>, Alejandro Rodríguez Cristo<sup>b</sup>, Adrian Paz Ramos<sup>c</sup>, Rafael Quintana Puchol<sup>d</sup>

<sup>a</sup> Biomaterials Center, University of Havana, Universidad Avenue and G, Havana, Cuba

<sup>b</sup> Mechanical Plants Company, Road of the Sub-Plant, Farm La Cana, Santa Clara, Villa Clara, Cuba

<sup>c</sup> Department of Chemistry, Université de Montréal, Succursale Centre-Ville, Montréal, Québec, Canada

<sup>d</sup> Welding Research Center, Central University Marta Abreu of Las Villas, Road to Camajuani km 5 1/2, Santa Clara, Villa Clara, Cuba

Received: April 18, 2016; Revised: October 18, 2016; Accepted: November 21, 2016

The chromium carbide coatings are widely used in the mechanical industry due to its corrosion resistance and mechanical properties. In this work, we evaluated a new source of chromium and silicon with micro-additions of boron on the deposition of multi-component coatings of chromium carbides in W108 steel. The coatings were obtained by the pack cementation method, using a simultaneous deposition at 1000 °C for 4h. The coatings were analyzed by X-ray diffraction, X-ray energy dispersive spectroscopy, optical microscopy, microhardness test method and pin-on-disc wear test. It was found that the coatings formed on W108 steel were mainly constituted by  $(\text{Cr,Fe})_{23}\text{C}_6$ ,  $(\text{Cr,Fe})_7\text{C}_3$ ,  $\text{Cr}_{5-x}\text{Si}_x\text{C}_{x+2}$ ,  $\text{Cr}_3\text{B}_{0.44}\text{C}_{1.4}$  and (or)  $\text{Cr}_7\text{BC}_4$ . The carbide layers showed thicknesses between 14 and 15  $\mu\text{m}$  and maximum values of microhardness between 15.8 and 18.8 GPa. Also, the micro-additions of boron to the mixtures showed statistically significant influence on the thickness, microhardness and abrasive wear resistance of the carbide coatings.

**Keywords:** *Chrome–boronizing–siliconizing, chromizing, chromium carbide, multicomponent coating, chromite, pack cementation method*

### 1. Introduction

Cold-work tools are exposed to hard and complex work conditions (high loads, abrasive and adhesive wear, mechanical fatigue, etc.)<sup>1-2</sup>. This affects its durability, making necessary its replacement in shorter operating periods. Wear, in its various forms, has a key role in the lifetime of cold-work tools and machine components<sup>3</sup>. During the past decades, the ceramic coatings have been used for increasing the lifetime of forming tools, cutting tools and machine components<sup>4-5</sup>. These layers are mainly constituted by borides, carbides, nitrides and carbonitrides of transition metals<sup>4-7</sup>. Ceramic coatings of titanium compounds (TiN, TiC, and TiCN) are generally used for this purpose<sup>8-11</sup>. However, its cost is high due to the considerable value of titanium sources (titanium chloride, ferrotitanium, and metallic titanium), and the equipment employed in its manufacture. The chromium carbide coatings are well-known for its resistance to oxidation at high temperatures (< 700 °C) and relatively low cost. However, its use is limited due to its lower microhardness and abrasive wear resistance in comparison with the carbide layers, nitrides and carbonitrides of other transition elements. The micro-alloying of chromium carbide coatings with one or more elements (titanium, vanadium, boron, silicon, nitrogen, etc.) is one promising alternative to solve this problem<sup>6,12-19</sup>.

The chrome-boronizing process on steel is performed by successive or simultaneous deposition processes of

the elements forming the coating<sup>14,16,20</sup>. The simultaneous formation of coatings of diffusive chromium carbides alloy with boron is obtained by using high chromium and low boron content in the mixtures<sup>16</sup>. Generally, the chromium carbides coatings are obtained by physical vapor deposition (PVD), chemical vapor deposition (CVD), plasma spray, Molten-salt or pack cementation method<sup>21-28</sup>. The chromium-carrier sources used in the pack cementation method are mainly ferrochrome and metallic chromium<sup>12,29</sup>. In a previous study, we reported the reduction products of a concentrate of chromium ore concentrate for this purpose<sup>30</sup>. The aim of the present work is to evaluate the influence of different mixtures obtained from the aluminothermic reduction of a chromium ore concentrate and of  $\text{B}_2\text{O}_3$  on the characteristics of multi-component coatings of chromium carbides on W108 steel.

### 2. Experimental Procedure

#### 2.1. Materials

Tool steel (W108) was used as the substrate. The elemental compositions (wt. %) of W108 steel was: C = 0.76; Si = 0.38; Mn = 0.2; Cr = 0.19 and Fe balance. Ten samples of 20 mm in diameter and 2 mm in thickness were used in the metallographic investigation, while 32 cylindrical samples (7.8 mm in diameter and 10 mm in length) were prepared for abrasive wear resistance tests.

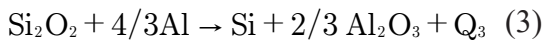
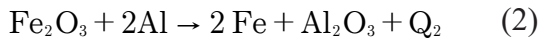
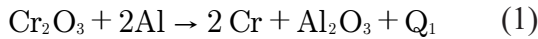
\* e-mail: [jesus.gonzalez@biomat.uh.cu](mailto:jesus.gonzalez@biomat.uh.cu)

A chromium ore concentrate from Cayo Guam was used as carrier source of chromium, silicon and inert filler in the diffusive process. The chemical composition (%) of this ore was:  $\text{Cr}_2\text{O}_3 = 35.48$ ;  $\text{SiO}_2 = 10.00$ ;  $\text{Al}_2\text{O}_3 = 19.92$ ;  $\text{CaO} = 0.52$ ;  $\text{MgO} = 17.68$ ;  $\text{Fe}_2\text{O}_3 = 13.65$ ;  $\text{TiO}_2 = 0.45$  and  $\text{MnO} = 0.17$ .

## 2.2 Mixtures composition and procedures

Three mixtures were used in the experiments (Table 1). The formation of the mixtures was divided into two stages: the first was the aluminothermic reduction process, followed by the addition of an activator ( $\text{NH}_4\text{Cl}$ ) to the resulting reduction products.

During the aluminothermic reduction of the oxides from chromium ore concentrate ( $\text{Cr}_2\text{O}_3$ ,  $\text{Fe}_2\text{O}_3$  and  $\text{SiO}_2$ ), and  $\text{B}_2\text{O}_3$ , the following chemical reactions were conducted, according to equations 1-4:



The chromium ore concentrate was mixed with aluminum powder (mixture 1, Table 1), while in mixtures 2 and 3 were also mixed with  $\text{B}_2\text{O}_3$  (mixture 2 and 3, Table 1). Then, the mixtures were put in reactors, sealed with a mixture of fireclay and sodium silicate and then subjected to reduction process at  $1000^\circ\text{C}$  for 4 h. Subsequently, the resulting products were grounded in a ball mill and sieved until obtaining a particle size of  $200\ \mu\text{m}$  or less. Diffusive treatments were also performed at  $1000^\circ\text{C}$  for 4 h, using a similar procedure to that reported in previous work<sup>30</sup>.

## 2.3 Characterization of the material and coatings

The chemical composition of the steel used as substrate was determined using a metal analyzer (Spectrolab, Germany). The average of three tests for each chemical element was determined. The aluminothermic reduction products were characterized using an X-ray diffractometer Phillips PW 1218, using the targeting method in accordance with Bragg – Brentano configuration. All spectra were obtained using a  $\text{FeK}\alpha 1$  ( $\lambda = 1.93604\ \text{\AA}$ ) radiation, filtered with Mn, a

current of 20 mA, a voltage of 30 kV, and an angular range ( $2\theta$ ) between  $7 - 60^\circ$ .

The elemental composition of the cross-section of carbide layers was determined using X-ray energy dispersive spectroscopy (EDS). The tests for the phase identification of the coating were carried out using an X-ray diffractometer Phillips PW 1710 with  $\text{CuK}\alpha$  radiation filtered with nickel.

Cross-sections of chromizing and chrome–boronizing–silicizing samples were metallographically prepared to observe the morphological details using a PMT-3 micro-Vickers hardness tester. The microhardness of the layers was measured at the cross-sections using a Micro-Vickers indenter (PMT – 3) with 20 g loads. Ten measurements of this parameter were performed for each sample. The samples for microscopy were prepared by standard metallographic techniques and etched in an alcoholic solution ( $\text{EtOH}/1\% \text{HNO}_3$ ).

Pin-on-disk test was used to study the abrasive wear resistance of coatings. 32 samples of W108 steels (as pin) with and without coating were used in the test. Also, samples of the same steel and hardened in water ( $800^\circ\text{C}$ ) and low tempered ( $180^\circ\text{C}$ ), were included. Eight samples were used for each experimental run. The parameters employed in this test are shown in Table 2.

## 2.4 Statistical analysis

Layer thickness, maximum microhardness value, and wear volume values were reported as an average  $\pm$  standard deviation. A one-way analysis of variance (ANOVA) and multiple sample comparisons test were carried out. Differences of  $p < 0.05$  were considered to be statistically significant.

# 3. Results and discussion

## 3.1 Effect of the reduction process of the chromium concentrate

Figure 1 shows the XRD patterns of the products obtained by aluminothermic reduction process using two different chromium/boron ratios.

The peaks corresponding to complex oxides of chromium and iron (chromopicotite) or silicon (antigorite) show relative low intensity, or they are not observed (Figure 1 A and B). The chromopicotite, at the interplanar distance of  $4.76\ \text{\AA}$ , is not revealed, while the peaks at  $2.902 - 2.919$ ;  $2.489$  and  $2.050 - 2.064\ \text{\AA}$  show a low relative intensity. These

**Table 1:** Mixture composition.

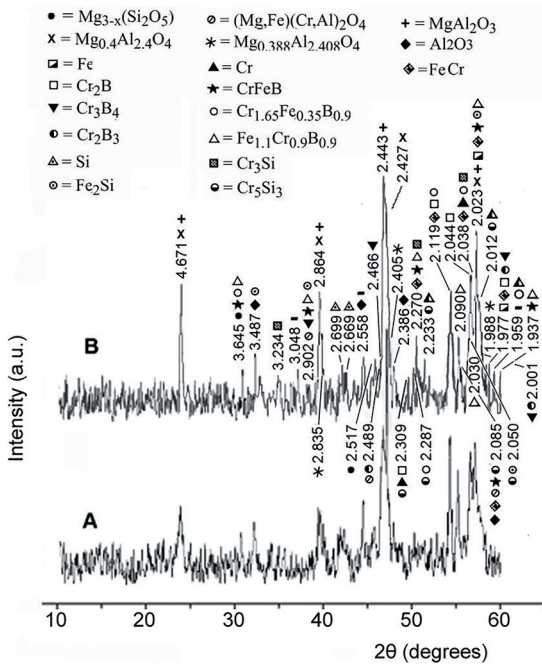
Mixture	Composition	Cr/B Ratio
1	98 % [54.5 % chromite* + 24.2 % $\text{Cr}_2\text{O}_3$ + 21.3 % aluminum]** + 2 % $\text{NH}_4\text{Cl}$	-----
2	98 % [54.1 % chromite* + 24 % $\text{Cr}_2\text{O}_3$ + 0.9 % $\text{B}_2\text{O}_3$ + 21 % aluminum]** + 2 % $\text{NH}_4\text{Cl}$	107/1
3	98 % [52.1 % chromite* + 24 % $\text{Cr}_2\text{O}_3$ + 1.9 % $\text{B}_2\text{O}_3$ + 22 % aluminum]** + 2 % $\text{NH}_4\text{Cl}$	50/1

\* Chromium ore concentrate, \*\*Aluminothermic reduction products.

**Table 2:** Parameters used in the pin-on-disk wear tests.

Pressure (MPa)	Velocity (m/s)	Time (s)	Abrasive
0.5	1.5	5	Silicon carbide disk (227- grit)*

\* Vickers Hardness = 20 – 30 GPa.

**Figure 1:** XRD diffraction patterns of the aluminothermic reduction products of the chromium ore concentrate from Cayo Guam deposit and  $B_2O_3$ . A - chromium/boron ratio = 107/1, B - chromium/boron ratio = 50/1.

peaks can be assigned to some phases obtained during the aluminothermic reduction. The peaks at the interplanar distances of 7.300 - 7.320; 3.645 - 3.659 and 2.517 - 2.502 Å are assigned to the antigorite ( $Mg_{3-x}(Si_2O_5)(OH)_{4-2x}$ ), a silicon-carrier phase.

### 3.1.1 Refractory products of the reduction

The refractory oxides  $MgAl_2O_4$ ,  $Mg_{0.4}Al_{2.4}O_4$  and (or)  $(Mg_{0.37}Al_2)O_4$  are presented in the reduction products of the mixtures with micro-addition of boron (Figure 1 A and B). The peaks with interplanar distances of 4.671 to 4.678, 2.849 to 2.864, 2.830 to 2.832, 2.441 to 2.443, from 2.417 to 2.427, from 2.405 to 2.407 and from 1.987 to 1.988 Å are assigned to those phases. Spinel is a phase resulting from the reduction of chromopicotite and antigorite, and they are present due to a new structural arrangement and interactions of the reaction products. In general, the peaks with high relative intensity in the XRD patterns of reduction products correspond to those phases. This result agrees with the contents of aluminum

and magnesium in the mixtures and is also an indicator that the effective reduction process of the chromium ore was carried out. The peaks at the interplanar distances of 3.486, 2.556, 2.396 and 2.087 Å are assigned to alumina ( $Al_2O_3$ ).

### 3.1.2 Phase carriers of the coating elements

Elements that can potentially contribute to the coating formation are detected in both mixtures in its elemental (metallic) or compound form (Figure 1 A and B). The peaks with interplanar distances of 2.304-2.309 and 2.038 Å can be assigned to chromium, while the peaks at 2.260-2.270, 2.119-2.120, 2.085-2.089, 2.038, 2.024-2.025, 1.970-1.977 and 1.937 Å are assigned to ferrochrome.

In both XRD patterns are revealed the presence of boron compounds. The peaks with interplanar distances of 1.937, 1.955 to 1.959, 1.970-1.977, 2.009-2.012, 2.024-2.025, 2.038, 2.041-2.047, 2.119-2.120, 2.304-2.309, 2.451-2.468, 2.489, 2.556-2.558, 2.902-2.919, 3.046-3.056 Å are assigned to compounds of boron - chromium ( $Cr_2B$ ,  $Cr_3B_4$ ,  $Cr_2B_3$  and  $CrB_2$ ) (Figure 1 A and B). Furthermore, some peaks can be assigned to chromium - iron boride ( $Cr_{1.65}Fe_{0.35}B_{0.9}$ ,  $Fe_{1.1}Cr_{0.9}B_{0.9}$  and  $Cr,Fe,B$ ) at the interplanar distances of 1.937, 1.955 to 1.959, 2.024-2.025, 2.038, 2.030-2.034, 2.085-2.089, 2.090-2.097, 2.119-2.120, 2.260-2.270, 2.279-2.287, 2.902-2.919 and 3.645-3.659 Å (Figure 1 A and B). In general, it can be noticed a higher relative intensity of the peaks corresponding to boron compounds in the diffractograms of the mixture with a chromium/boron ratio = 50/1 (Figure 1 B). This result agrees with the highest content of boron introduced into the above-mentioned mixture.

In the XRD patterns, some peaks can also be assigned to silicon and silicon compounds with chromium ( $Cr_3Si$  and  $Cr_5Si_3$ ), with iron ( $Fe_2Si$ ) and with chromium - iron ( $Cr_{0.78}Fe_{2.22}Si_2$ ) (Figure 1 A and B).

## 3.2. Characterization of the coatings

### 3.2.1 Elemental and phase composition

EDS tests of the chromizing and chrome-boronizing-silicizing samples show the presence of chromium and iron in the coatings (Figure 2 A and B). Also, low contents of silicon are detected in the chrome-boronizing-silicizing layer (Figure 3).

The elemental composition of the coatings changed in its cross section, showing the highest contents of chromium in the surface of the coatings (Figure 3). It is also noticeable two different areas by its chromium content. The first area (carbides layer, near to the surface) have a chromium content between 72 – 40% (chromizing layer, not shown) and 87 - 43% (chrome-boronizing-silicizing layer, zone I in Figure

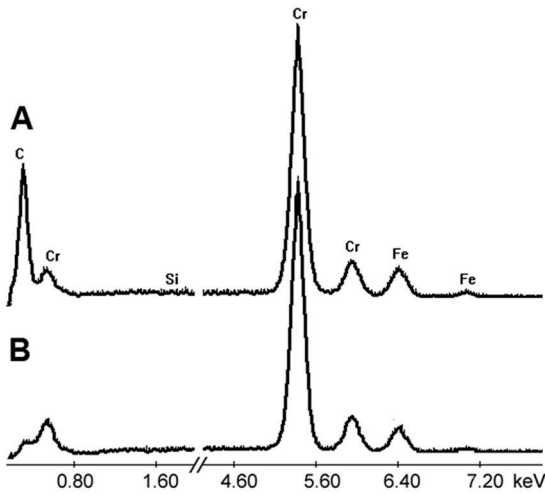


**Figure 2:** EDS spectra of the coatings surface. A - Chromizing, B - Chrome-boronizing-siliconizing (obtained using the mixture 3).

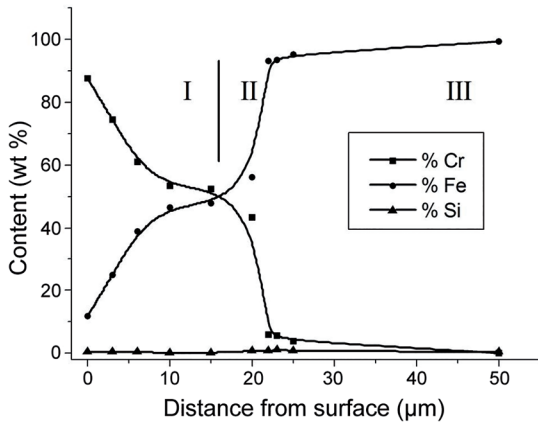


**Figure 3:** Concentration profiles of chromium, iron and silicon (by EDS) in the cross section of a sample chrome-boronizing-siliconizing (obtained using the mixture 3).

3). In the second area, (transition zone next to the carbides coating; II in Figure 3) the chromium content decreases progressively towards the substrate (zone III, Figure 3). In addition, silicon content in the chrome-boronizing-siliconizing coatings changed, reaching its maximum concentration in the transition zone (0.64 – 1.12%).

The diffusive treatment applied to W108 steel using mixtures 1 (for chromizing) and 2 (with chromium/boron ratio = 107/1) allow to obtain chromium carbide coatings (Figure 4).

The number of major peaks in the XRD patterns of both coatings are assigned to chromium-iron carbides ((Cr, Fe)<sub>23</sub>C<sub>6</sub> and Cr, Fe<sub>7</sub>C<sub>3</sub>, with interplanar distances of: 1.140, 1.170, 1.180, 1.185 - 1.186, 1.201 - 1.205; 1.254; 1.343, 1.455, 1.601 - 1.607, 1.756, 1.805, 1.882 - 1.890, 2.031 - 2.048 and 2.110 Å) and (or) chromium - silicon (Cr<sub>5-x</sub>Si<sub>3-x</sub>C<sub>x+z</sub>, interplanar distances of: 1.180 - 1.185, 1.201 - 1.205, 1.250, 1.310, 1.342 - 1.343, 1.505 - 1.516, 1.660, 1.869, 1.950 - 1.975, 2.031 - 2.040, and 2.339 Å) (Figure 4).

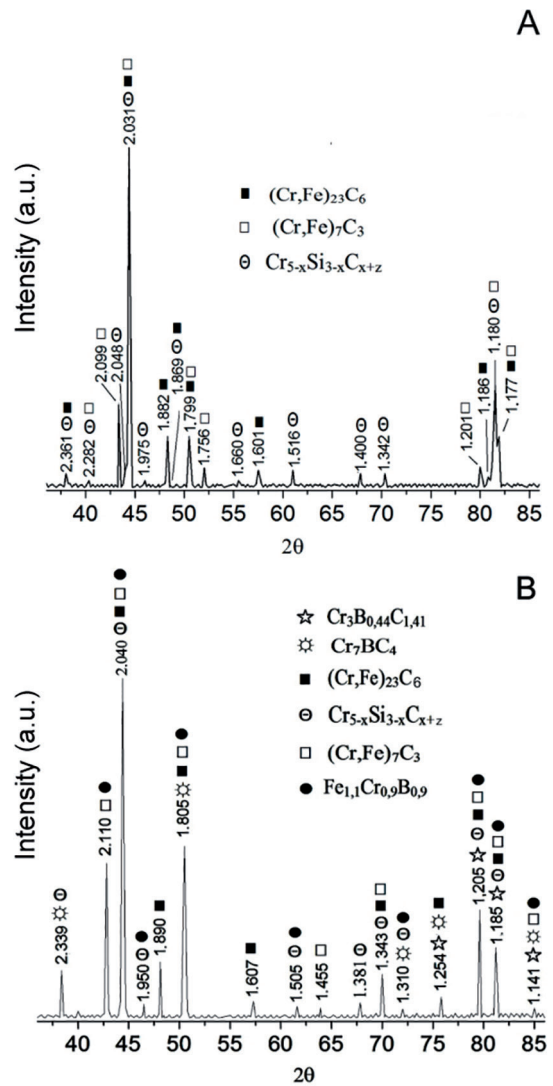


**Figure 4:** XRD diffraction patterns of the coatings. A) - Chromizing and B) - Chrome-boronizing-siliconizing (obtained using the mixture 2).

The XRD patterns of the chrome-boronizing-siliconizing samples show new phases at the interplanar distances of 1.141, 1.254, 1.310 and 2.339 Å. These peaks can be assigned to the chromium-boron carbide(s) Cr<sub>3</sub>B<sub>0,44</sub>C<sub>1,4</sub> and (or) Cr<sub>7</sub>BC<sub>4</sub>. The chromium-boron carbide can also be overlapped with the peaks at the interplanar distances of 1.185, 1.205 and 1.805 Å. Moreover, the main peaks that identify the chromium-iron boride Fe<sub>1,1</sub>Cr<sub>0,9</sub>B<sub>0,9</sub> are in agreement with those previously assigned to different complex carbides (interplanar distances of 1.114, 1.185, 1.205, 1.310, 1.505, 1.805, 1.950, 2.040 and 2.110 Å) (Figure 4).

### 3.2.2 Morphology, thickness and microhardness of the coatings

The cross section of the coatings obtained on W108 steel using mixtures without (mixture 1) and with micro-addition of boron (mixture 3) showed a uniform carbides layer

(zone I, Figure 5A and 5B). Besides, there is no significant difference in the morphology of the cross section of those carbide layers.

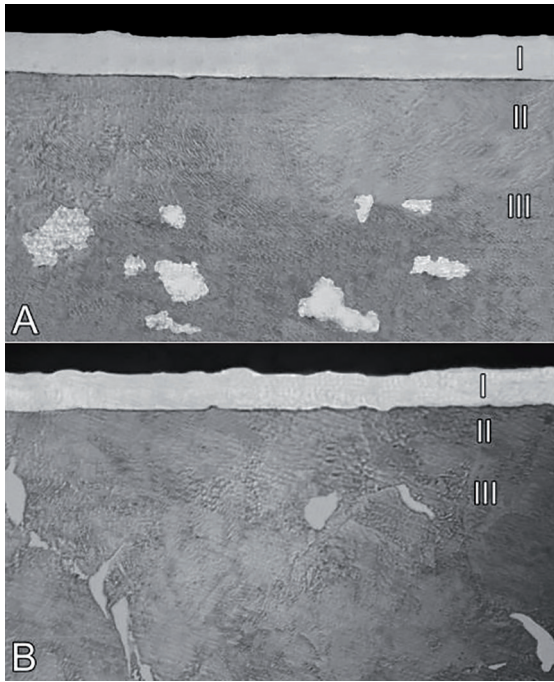


**Figure 5:** Cross-sectional morphology of the coatings (Optical Microscopy), 500 X. A - Chromizing, B - Chrome-boronizing-siliconizing (obtained using the mixture 3).

After the coating layer, it can be seen the substrate, which exhibits a pearlitic structure with a microhardness of 2.45 GPa and some inclusions of ferrite, which it does not typical of this steel in annealed condition. This region is located at 50 - 150  $\mu\text{m}$  from the surface (zone III, Figure 5 A and B). The above observation is probably linked to the reduction of carbon content due to the formation of the carbide layer. The transition zone is not clearly revealed and also does not show the ferritic area. The absence of this ferritic region is related to the diffusion of carbon from the substrate to the area near to the coating.

The chromizing and chrome-boronizing-siliconizing samples (obtained in a mixture with a chromium/boron ratio = 107/1) show similar layer thickness (Table 3). However, the coatings obtained using the mixture with a chromium/boron ratio = 50/1 shows statistically significant differences with the rest of coatings (Table 3). The reduction of this parameter is around 6% in comparison with the chromizing layers. In previous work, Chen *et al.*<sup>16</sup> reported a decrease in the carbides layer thickness of chrome-boronizing-siliconizing samples compared to chromizing layers.

In general, we observe a decrease in the thickness of the carbide layers with the increase of the boron content in the mixtures. This fact may be linked to the formation of

stable compounds in the mixture due to reactions between the active elements. As well, it can be related to the kinetics of the reactions between those elements and the activator.

The coatings show different microhardness values at the cross section (Figure 6), a behavior that could be related to variations in its elemental and phase composition. The maximum values of this parameter were found in the middle area of its cross-section ( $15.80 \pm 0.17$  to  $18.79 \pm 0.15$  GPa), and its magnitude depends on the boron content in the saturating mixture. In the area near to the surface of the coating, the microhardness is slightly lower than the remaining zones (Figure 6). This behavior must be related to a higher content of the phase  $(\text{Cr,Fe})_{23}\text{C}_6$  in this area. Li *et al.*<sup>31</sup> found that the phase  $(\text{Cr,Fe})_{23}\text{C}_6$  has a lower microhardness than the carbide  $(\text{Cr,Fe})_7\text{C}_3$ , thus it can affect to some extent the mechanical properties at the surface.

The chrome-boronizing-siliconizing samples show statistically significant differences in the maximum microhardness values with respect to chromizing coatings. In general, boron additions to the mixtures resulted in increments of between 1.86 and 3.09 GPa in the maximum microhardness values (Figure 6, Table 3). The maximum microhardness values of the chrome-boronizing-siliconizing coatings are similar to those reported by Chen *et al.*<sup>16</sup> for a multi-components layer (chrome-boronizing-siliconizing, mixtures h and g) on medium-carbon steel. Also, they are higher than those obtained in previous works for chromizing layers<sup>30</sup>.

### 3.2.3. Abrasive wear test

The abrasion tests of the coatings generate crests and valleys oriented in the direction of the abrasive displacement. The morphology of the samples before and after the test is shown in Figure 7.

The chromizing and chrome-boronizing-siliconizing coatings show statistically significant differences in its wear volume in comparison with the W108 steel hardened and low tempered (Figure 8).

The coating obtained using the mixture 3 (with a chromium/boron ratio = 50/1) shows statistically significant differences in the wear volume in comparison with the rest of the coatings, while there are not differences between the coating obtained using mixture 2 (with a chromium/boron ratio = 107/1) and the chromizing layer. These results are related to the high microhardness values of the carbide layers in the chrome-boronizing-siliconizing samples.

## 4. Conclusion

In this work, the aluminothermic reduction products of mixtures of chromium ore concentrate and  $\text{B}_2\text{O}_3$  were obtained. XRD analysis allows the identification of refractory compounds (aluminum oxide and spinels) and active elements (chromium, iron, silicon, boron and (or) its compounds).

**Table 3:** Coating thickness and maximum microhardness value in the cross section of the carbide layers.

Mixture	Thickness ( $\mu\text{m}$ )	SD*	VC ** (%)	Microhardness (GPa)	SD	VC (%)
1	15.00	0.19	1.24	15.80	0.17	0.75
2	15.15	0.19	1.23	17.56	0.16	0.92
3	14.02	0.25	1.79	18.79	0.15	0.79

\* Standard deviation, \*\* Variation coefficient

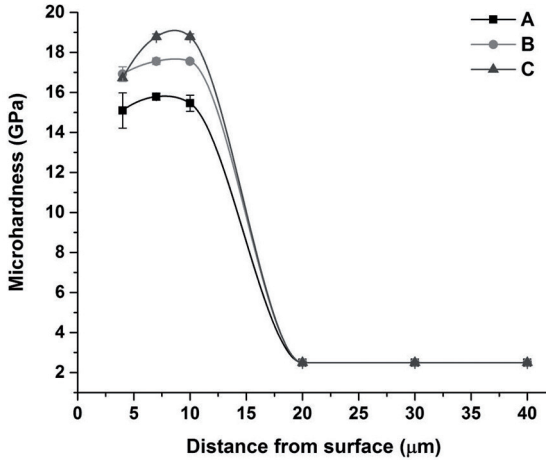


**Figure 6:** Cross-sectional microhardness profiles. A - Chromizing, B - Chrome-boronizing-siliconizing (obtained using the mixture 2) and C - Chrome-boronizing-siliconizing (obtained using the mixture 3).

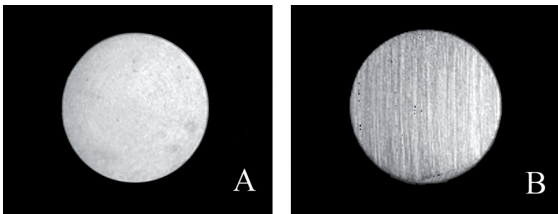


**Figure 7:** Morphology (Optical Microscopy) of the surfaces before (A) and after (B) the pin-on-disk wear test.

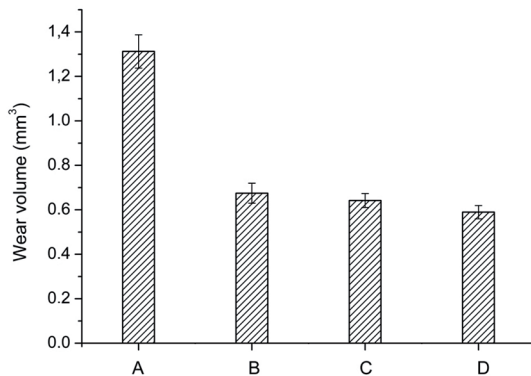


**Figure 8:** Wear volume. A - Heat treatment, B - Chromizing, C - Chrome-boronizing-siliconizing (obtained using mixture 2) and D - Chrome-boronizing-siliconizing (obtained using mixture 3).

The active elements and its compounds allow its use for the further production of chromium carbide coatings by pack cementation method.

The chrome-boronizing-siliconizing process on W108 steel was successfully performed. Multi-components coatings of complex chromium-iron carbides ( $(\text{Cr,Fe})_{23}\text{C}_6$  and  $(\text{Cr,Fe})_7\text{C}_3$ ), chromium-silicon ( $\text{Cr}_{5-x}\text{Si}_{3-x}\text{C}_{x+2}$ ) and chromium-boron ( $\text{Cr}_3\text{B}_{0.44}\text{C}_{1.4}$  and (or)  $\text{Cr}_7\text{BC}_4$ ) were obtained. These layers were characterized by a thickness of 14 - 15  $\mu\text{m}$ , a maximum chromium content of around 87%, maximum microhardness values between 15.7 - 18.79 GPa, and a high abrasive wear resistance.

The chromium/boron ratios showed statistically significant influence on the thickness, microhardness and abrasive wear resistance of the coatings. Indeed, the higher microhardness value and abrasive wear resistance of the chromium carbide layers on W108 steel were obtained using mixtures with chromium-boron ratio = 50/1. The chrome-boronizing-siliconizing coating had higher abrasive wear resistance than the chromizing layer and the hardened and low tempered W108 steel.

## 5. References

- Wagner K, Putz A, Engel U. Improvement of tool life in cold forging by locally optimized surfaces. *Journal of Materials Processing Technology*. 2006;177(1-3):206-209.
- Lee YC, Chen FK. Failure analysis of a cold-extrusion punch to enhance its quality and prolong its life. *Journal of Materials Processing Technology*. 2000;105(1-2):134-142.
- Sen S. Influence of chromium carbide coating on tribological performance of steel. *Materials & Design*. 2006;27(20):85-91.
- Lajtin Y, Arzamazov B. Tratamiento Químico-Térmico de los Metales. Moscow: Editorial Mir; 1987.
- Su YL, Liu TH, Su CT, Yur JP, Kao WH, Yao SH. Tribological characteristics and cutting performance of  $\text{Cr}_x\text{C}$ -coated carbide tools. *Journal of Materials Processing Technology*. 2004;153-154:699-706.
- Sen S, Sen U. The effect of boronizing and boro-chromizing on tribological performance of AISI 52100 bearing steels. *Industrial Lubrication and Tribology*. 2009;61(3):146-153.
- Taktak S, Ulker S, Gunes I. High temperature wear and friction properties of duplex surface treated bearing steels. *Surface and Coatings Technology*. 2008;202(14):3367-3377.

8. Coronel E, Wiklund U, Olsson E. The effect of carbon content on the microstructure of hydrogen-free physical vapour deposited titanium carbide films. *Thin Solid Films*. 2009;518(1):71-76.
9. Guu YY, Lin JF, Ai CF. The tribological characteristics of titanium nitride, titanium carbonitride and titanium carbide coatings. *Thin Solid Films*. 1997;302(1-2):193-200.
10. Sen U. Friction and wear properties of thermo-reactive diffusion coatings against titanium nitride coated steels. *Materials & Design*. 2005;26(2):167-174.
11. Zeghni AE, Hashmi MSJ. Comparative wear characteristics of tin and tic coated and uncoated tool steel. *Journal of Materials Processing Technology*. 2004;155-156:1923-1926.
12. Hakami F, Sohi MH, Ghani JR. Duplex surface treatment of AISI 1045 steel via plasma nitriding of chromized layer. *Thin Solid Films*. 2011;519(20):6792-6796.
13. Harper MA, Rapp RA. Codeposited chromium and silicon diffusion coatings for Fe-Base alloys via pack cementation. *Oxidation of Metals*. 1994;42(3):303-333.
14. Karpman MG, Sokolova NK, Nikolaev GS. Protective coatings for dies and die-casting molds for nonferrous casting. *Metal Science and Heat Treatment*. 1977;19(9):794-797.
15. Polcar T, Vitu T, Cvrcek L, Vyskocil J, Cavaleiro A. Effects of carbon content on the high temperature friction and wear of chromium carbonitride coatings. *Tribology International*. 2010;43(7):1228-1233.
16. Chen FS, Wang KL. The kinetics and mechanism of multi-component diffusion on AISI 1045 steel. *Surface and Coatings Technology*. 1999;115(2-3):239-248.
17. Hu ZQ, Tan GH, Zeng XT, Ding XZ. Thermal stability of CrCO-Ti compound coating. *Thin Solid Films*. 2008;516(8):1906-1912.
18. Cheng F, Wang Y, Yang T. Microstructure and wear properties of Fe-VC-Cr<sub>7</sub>C<sub>3</sub> composite coating on surface of cast steel. *Materials Characterization*. 2008;59(4):488-492.
19. Khalaj G, Nazari A, Khoie SMM, Khalaj MJ, Pouraliakbar H. Chromium carbonitride coating produced on DIN 1.2210 steel by thermo-reactive deposition technique: Thermodynamics, kinetics and modeling. *Surface and Coatings Technology*. 2013;225:1-10.
20. Lee SY, Kim GS, Kim BS. Mechanical properties of duplex layer formed on AISI 403 stainless steel by chromizing and boronizing treatment. *Surface and Coatings Technology*. 2004;177:178-184.
21. Cao H, Wu C, Liu J, Luo C, Zou G. Novel duplex low-temperature chromizing process at 500°C. *Journal of Materials Science & Technology*. 2007;23(6):823-827.
22. Bai CY, Wen TM, Hou KH, Ger MD. The bipolar plate of AISI 1045 steel with chromized coatings prepared by low-temperature pack cementation for proton exchange membrane fuel cell. *Journal of Power Sources*. 2010;195(3):779-786.
23. Lin N, Xie F, Wu X, Tian W. Influence of process parameters on thickness and wear resistance of rare earth modified chromium coatings on P110 steel synthesized by pack cementation. *Journal of Rare Earths*. 2011;29(4):396-400.
24. Chen X, Peng Z, Fu Z, Yue W, Yu X, Wang C. Influence of individual Cr-C layer thickness on structural and tribological properties of multilayered Cr-C/a-C:Cr thin films. *Surface and Coatings Technology*. 2010;204(20):3319-3325.
25. Henderer W, Xu F. Hybrid TiSiN, CrC/C PVD coatings applied to cutting tools. *Surface and Coatings Technology*. 2013;215:381-385.
26. Staia MH, Suárez M, Chicot D, Lesage J, Iost A, Puchi-Cabrera ES. Cr<sub>2</sub>C<sub>3</sub>-NiCr VPS thermal spray coatings as candidate for chromium replacement. *Surface and Coatings Technology*. 2013;220:225-231.
27. Ziebert C, Ye J, Stüber M, Ulrich S, Edinger M, Barzen I. Ion bombardment-induced nanocrystallization of magnetron-sputtered chromium carbide thin films. *Surface and Coatings Technology*. 2011;205(2):4844-4849.
28. Betts JC, Mordike BL, Fenech M, Grech M. Direct laser deposition and sliding wear of AISI316/WC10Ni and AISI316/Cr<sub>3</sub>C<sub>2</sub> surfaces. *Surface Engineering*. 2009;25(2):167-176.
29. Behrani VR, Singh PM. Corrosion behavior of aluminized and chromized carbon steel in fluctuating oxidizing-sulfidizing environments. In: *NACE - International Corrosion Conference Series*; 2007 March 11-15; Nashville, TN, USA.
30. González Ruiz JE, Quintana Puchol R, Rodríguez Cristo A, Duffus Scout A. Evaluación de los productos de la reducción de un concentrado cromífero en la obtención de recubrimientos difusivos de carburos de cromo. *Revista CENIC de Ciencias Químicas*. 2009;40(3):143-148.
31. Lin CM, Chang CM, Chen JH, Wu W. Hardness, toughness and cracking systems of primary (Cr,Fe)<sub>23</sub>C<sub>6</sub> and (Cr,Fe)<sub>7</sub>C<sub>3</sub> carbides in high-carbon Cr-based alloys by indentation. *Materials Science and Engineering: A*. 2010;527(18-19):5038-5043.